An Odd Oxygen Framework for Wintertime Ammonium Nitrate Aerosol Pollution in Urban Areas: NOx and VOC Control as Mitigation Strategies

C. C. Womack[1,2] (iD), E. E. McDuffie[1,2,3,4] (iD), P. M. Edwards[5] (iD), R. Bares[6] (iD), J. A. de Gouw[2,3] (iD), K. S. Docherty[7], W. P. Dubé[1,2], D. L. Fibiger[1,2,8] (iD), A. Franchin[1,2] (iD), J. B. Gilman[1] (iD), L. Goldberger[9,10], B. H. Lee[9] (iD), J. C. Lin[6] (iD), R. Long[11], A. M. Middlebrook[1], D. B. Millet[12] (iD), A. Moravek[13,14] (iD), J. G. Murphy[13] (iD), P. K. Quinn[15], T. P. Riedel[11] (iD), J. M. Roberts[1] (iD), J. A. Thornton[9] (iD), L. C. Valin[11] (iD), P. R. Veres[1] (iD), A. R. Whitehill[11], R. J. Wild[1,2,16] (iD), C. Warneke[1,2] (iD), B. Yuan[1,2,17], M. Baasandorj[6,18], and S. S. Brown[1,3] (iD)

[1]Chemical Sciences Division, NOAA Earth System Research Laboratory, Boulder, CO, USA, [2]Cooperative Institute for Research in Environmental Sciences, University of Colorado Boulder, Boulder, CO, USA, [3]Department of Chemistry, University of Colorado Boulder, Boulder, CO, USA, [4]Now at the Department of Physics and Atmospheric Science, Dalhousie University, Halifax, Nova Scotia, Canada, [5]Department of Chemistry, University of York, York, UK, [6]Department of Atmospheric Sciences, University of Utah, Salt Lake City, UT, USA, [7]Jacobs Technology, Inc., Durham, NC, USA, [8]Now at California Air Resources Board, Sacramento, CA, USA, [9]Department of Atmospheric Sciences, University of Washington, Seattle, WA, USA, [10]Now at ARM Aerial Facility, Pacific Northwest National Laboratory, Richland, WA, USA, [11]Office of Research and Development, Environmental Protection Agency, Durham, NC, USA, [12]Department of Soil, Water, and Climate, University of Minnesota, Twin Cities, St. Paul, MN, USA, [13]Department of Chemistry, University of Toronto, Toronto, Ontario, Canada, [14]Now at Department of Chemistry, York University, Toronto, Ontario, Canada, [15]NOAA Pacific Marine Environmental Laboratory, Seattle, WA, USA, [16]Now at the Institut für Ionenphysik und Angewandte Physik, Universität Innsbruck, Innsbruck, Austria, [17]Now at the Institute for Environmental and Climate Research, Jinan University, Guangzhou, China, [18]Division of Air Quality, Utah Department of Environmental Quality, Salt Lake City, UT, USA

Abstract Wintertime ammonium nitrate aerosol pollution is a severe air quality issue affecting both developed and rapidly urbanizing regions from Europe to East Asia. In the United States, it is acute in western basins subject to inversions that confine pollutants near the surface. Measurements and modeling of a wintertime pollution episode in Salt Lake Valley, Utah, demonstrate that ammonium nitrate is closely related to photochemical ozone through a common parameter, total odd oxygen, $O_{x,total}$. We show that the traditional nitrogen oxide and volatile organic compound (NOx-VOC) framework for evaluating ozone mitigation strategies also applies to ammonium nitrate. Despite being nitrate-limited, ammonium nitrate aerosol pollution in Salt Lake Valley is responsive to VOCs control and, counterintuitively, not initially responsive to NO_x control. We demonstrate simultaneous nitrate limitation and NO_x saturation and suggest this phenomenon may be general. This finding may identify an unrecognized control strategy to address a global public health issue in regions with severe winter aerosol pollution.

Plain Language Summary Particulate matter (PM) is dangerous to human health and impacts visibility and climate. In the United States, Europe, and Asia, PM is severe in urban areas in the winter when ammonium nitrate, NH_4NO_3, comprises an appreciable fraction of the total PM mass. A key control strategy is to reduce emissions of the limiting reagent. Using measurements from a recent field campaign in the Salt Lake Valley, Utah, which experiences high PM levels in winter, we demonstrate that emission control strategies can be evaluated using the same framework commonly used to control ozone, another common pollutant that occurs at high levels in urban areas in the summer. We show that initial control of the NO_x precursor is ineffective at reducing NH_4NO_3 aerosol in the Salt Lake Valley, while initial control of volatile organic compounds, which are not a direct precursor for either nitrate or ammonium, is effective due to their influence on oxidation cycles. This finding differs from many mitigation strategies in the western United States and may also be relevant to other regions in Europe and Asia which experience high wintertime PM.

1. Introduction

Air quality in most of the United States has been steadily improving for decades due to emissions control technologies and regulations (Hand et al., 2014). Ozone (O_3), which is a health hazard and greenhouse gas in the troposphere, has decreased markedly (Cooper et al., 2014) and is well understood in terms of its photochemical formation mechanism from nitrogen oxides ($NO_x = NO + NO_2$) and volatile organic compounds (VOCs; Lin et al., 1988; Seinfeld, 1989). In contrast, many urban areas, such as the Salt Lake Valley (SLV) and San Joaquin Valley in the western United States, the Po Valley in Europe, and Beijing, China, in east Asia, experience severe wintertime pollution in the form of particulate matter smaller than 2.5 microns in diameter ($PM_{2.5}$; Green et al., 2015; Figure 1). The SLV in northern Utah regularly experiences episodes of $PM_{2.5}$ pollution (Silcox et al., 2012), exacerbated by the onset of persistent cold air pools (PCAPs; high-pressure systems that cap colder air within the basin), which prevent the vertical mixing of pollutants away from the surface (Whiteman et al., 2014). The trapped gas-phase pollutants, including NO_x and VOCs from anthropogenic sources, undergo complex chemical oxidation reactions, forming nitric acid (HNO_3) that reacts with gas-phase ammonia (NH_3) to form ammonium nitrate aerosol (NH_4NO_3), which comprises ~75% of the $PM_{2.5}$ composition in the SLV during pollution episodes (Baasandorj et al., 2017; Franchin et al., 2018; Kuprov et al., 2014).

$$NH_3(g) + HNO_3(g) \leftrightarrows NH_4NO_3(aq). \tag{R1}$$
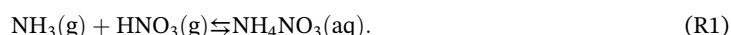
The SLV exceeds the 24-hr U.S. National Ambient Air Quality Standard for $PM_{2.5}$ (35 $\mu g/m^3$) on an average of 18 days/year (Whiteman et al., 2014), representing an important public health issue (Beard et al., 2012). A better understanding of the chemical processes that lead to the formation of ammonium nitrate and its precursors in the SLV and other polluted areas across the world is required to employ more effective control strategies.

Previous studies have demonstrated that during PCAP-induced pollution events, the valleys in the Salt Lake region typically have an excess of ammonia (Franchin et al., 2018; Kelly et al., 2013; Kuprov et al., 2014), and that the cold temperatures and high relative humidity drive the reversible reaction (R1) to form particulate ammonium nitrate (abbreviated pNO_3^-; Blanchard et al., 2000; Franchin et al., 2018; Weber et al., 2016). The recent analysis of Franchin et al. (2018) demonstrates that the observed ratio between gas-phase nitric acid and total nitrate, $HNO_3/(HNO_3 + pNO_3^-)$, has a median value of <8% during PCAP episodes, and the calculated aerosol pH curve is insensitive to small changes in pH (supporting information Figure S1). Furthermore, Franchin et al. (2018) show that the initial response of total aerosol mass to reductions in total nitrate ($HNO_3 + pNO_3^-$) is linear but substantially less than linear in its initial response to reductions in total reduced nitrogen ($NH_3 + NH_4^+$). Therefore, the formation rate of pNO_3^- is mainly limited by the chemical formation rate of nitric acid (HNO_3) from oxidation of NO_x, which is emitted from fossil fuel combustion. This HNO_3 limitation has led typical western U.S. control strategies to focus on emission reductions of NO_x rather than NH_3 (Franchin et al., 2018; Kelly et al., 2018; Pusede et al., 2016). We demonstrate in this study that ammonium nitrate aerosol pollution may be treated in the same manner as O_3 pollution through a common parameter, $O_{x,total}$, and may be most effectively reduced in the SLV by initially controlling VOC emissions rather than controlling emissions of NH_3 or NO_x.

2. Methods

2.1. Observations of Wintertime Pollution Episodes in Northern Utah

The Utah Winter Fine Particulate Study (UWFPS) was a 4-week field campaign in the SLV region during the winter of 2016–2017 designed to observe the chemical processes that form ammonium nitrate aerosol during PCAPs (Baasandorj et al., 2018; Bares et al., 2018; Franchin et al., 2018). Ground sites made continuous surface-level measurements of trace gases (including O_3, NO_x, and VOCs) and the chemical composition of $PM_{2.5}$, while a Twin Otter light aircraft made periodic measurements aloft with a similar payload. This analysis primarily uses observations from the main SLV site at the University of Utah (UU), with auxiliary measurements from the Hawthorne site on the SLV floor and the Logan site in the nearby Cache Valley (Figure S2). Two major PCAP episodes occurred during the campaign, in which the 24-hr $PM_{2.5}$ concentrations surpassed the National Ambient Air Quality Standard in at least one of the three major valleys for a
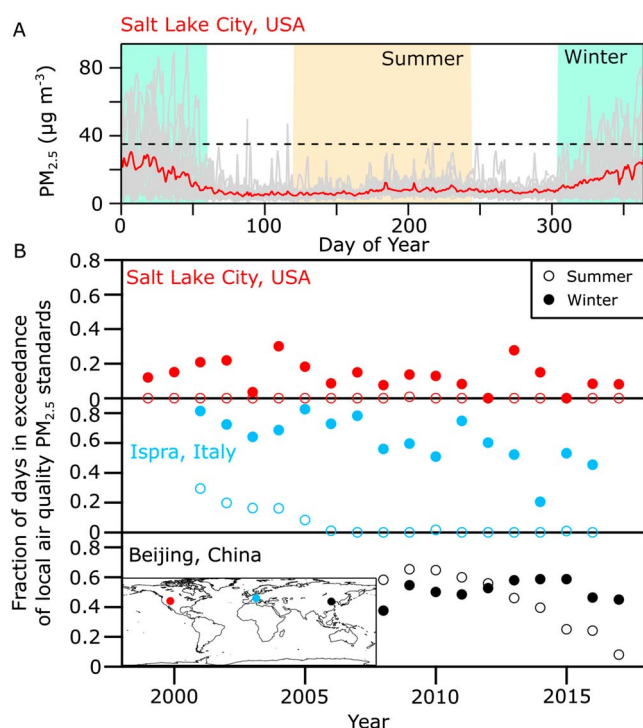
Figure 1. Seasonal trends in $PM_{2.5}$ nonattainment in three regions with high ammonium nitrate aerosol content. (a) Yearly profiles of $PM_{2.5}$ measured in the Salt Lake Valley, United States, between 1999 and 2017, with the average shown in red. Virtually all exceedances of the U.S. National Ambient Air Quality Standard (35 $\mu g/m^3$; dashed line) occur during the winter. (b) The fraction of winter and summer days in nonattainment of local air quality standards for $PM_{2.5}$ in the Salt Lake Valley (EPA, 2018), Ispra, Italy in the Po Valley (EMEP, 2018), and Beijing, China (DOS, 2018; see Text S1); these three regions are noted for their poor wintertime air quality and high ammonium nitrate aerosol mass loading. In the Salt Lake Valley and Po Valley, summertime exceedances are rare, while wintertime exceedances are persistent. In China, summertime exceedances have decreased in recent years, while wintertime exceedances remain frequent. $PM_{2.5}$ = particulate matter smaller than 2.5 microns in diameter.

total of 8 days. This analysis investigates the mechanisms for the $PM_{2.5}$ production that lead to the exceedance during one of the most intense pollution episode of that winter, which occurred between 27 January and 4 February 2017 (Figure S2). These results are compared to observations of trace gas species from the recent Uintah Basin Winter Ozone Study, where a major PCAP in January 2013 led to elevated levels of O_3 (Ahmadov et al., 2015; Edwards et al., 2014). Measurement techniques for both campaigns are described in detail in Text S1 (Lee et al., 2014; Liao et al., 2017; Wild et al., 2014; Wild et al., 2016).

2.2. $O_{x,total}$ as a Parameter for Describing both HNO_3 and O_3 Formation

There are two mechanisms for HNO_3 formation: daytime production from the gas-phase reaction of $OH + NO_2$ and nighttime production from N_2O_5 uptake onto aerosol particles (Jones & Seinfeld, 1983). The full mechanistic details are listed in Text S2 and summarized here. In the daytime, VOCs are photolyzed or oxidized by the hydroxyl radical (OH) to form HO_2 or RO_2 radicals, collectively termed HO_x radicals ($HO_x = OH + HO_2 + RO_2$). Radical propagation reactions with NO generate an NO_2 molecule with each iteration, while the dominant radical termination reaction of OH with NO_2 generates HNO_3. The overall HNO_3 production efficiency of this cycle depends on (1) the availability of HO_x radicals, which are generally less abundant in winter than in summer, and (2) the number of iterations each HO_x radical makes prior to termination (i.e., chain length), which is determined by the relative abundance of VOC and NO_x (Kleinman, 2005; Lin et al., 1988). During the day, NO_2 rapidly interconverts with NO and O_3, and therefore, the same HO_x cycle that produces HNO_3 is also the dominant mechanism for O_3 production. At night, photolytic production of radicals and O_3 halts, and NO titrates the O_3 to NO_2, which then oxidizes to form N_2O_5, which further reacts heterogeneously with aerosol to form HNO_3 and $ClNO_2$ (Kelly et al., 2018).

The parameter O_x (=$O_3 + NO_2$) has often been used to quantify the net photochemical formation of O_3 beyond its rapid daytime interconversion with NO_2 (Liu, 1977; Wood et al., 2009). Here we introduce an analogous parameter, $O_{x,total}$, which is equal to the sum of all gas- and particulate-phase species that contain an odd oxygen (O or O_3).

$$O_{x,total} = O_3 + NO_2 + 2 \times NO_3 + 3 \times N_2O_5 + ClNO_2 + \text{peroxyacyl nitrates} + 2 \times \text{alkyl nitrates} + OH + 1.5 \times (HNO_3 + pNO_3^-)), \tag{R2}$$

where the stoichiometric coefficients indicate the number of odd oxygen species it contains and are derived in Text S2. NH_3 is reduced nitrogen and is therefore not a component of $O_{x,total}$. The coefficient for the sum of gas-phase HNO_3 and pNO_3^- is denoted here as 1.5 but may be as high as 2, depending on the mechanism that formed it, and therefore, $O_{x,total}$ as defined here should be considered a lower bound. $O_{x,total}$ may be more broadly defined than (R2) if one considers the products of the reactions of OH, O_3, and NO_3 with VOCs, for example, but for this analysis, we focus only on the propagation of odd oxygen through nitrogen chemistry.

The nighttime mechanism results in no net change in $O_{x,total}$, as those reactions represent only a repartitioning of its components. The daytime mechanism, on the other hand, generates one NO_2 molecule for each cycle without loss of an O_3 molecule and therefore represents an increase in $O_{x,total}$ before terminating in HNO_3 or alkyl nitrate production. Transport of air masses with background concentrations of O_3 and negligible concentrations of the other $O_{x,total}$ components into the SLV would deplete the other $O_{x,total}$

components by their stoichiometric coefficients (≥ 1) for every O_3 molecule added, leading to a net decrease of $O_{x,total}$. Dry deposition of individual species to the surface is also a net loss process. Therefore, growth in $O_{x,total}$ beyond its background level in unpolluted air is a measure of the role that photochemistry plays in the net production of $HNO_3 + pNO_3^-$ during the PCAP.

2.3. Photochemical Box Modeling

The Dynamically Simple Model for Atmospheric Chemical Complexity (DSMACC) (Emmerson & Evans, 2009), a photochemical zero-dimensional box model, was used to characterize the growth of $O_{x,total}$ in the SLV during one of the most severe PCAPs sampled between 27 January and 4 February 2017. DSMACC utilizes the Master Chemical Mechanism (v3.3.1; Jenkin et al., 2015), a near-explicit mechanism to characterize the degradation of 143 VOCs by photochemistry and oxidation, using >15,000 reactions and >3,500 intermediate species. A subset of the Master Chemical Mechanism was used here, consisting of the 58 VOCs for which we had experimental constraints for the starting conditions. The Tropospheric Ultraviolet and Visible Radiation Model (v5.2; Madronich et al., 1998) was used to calculate the photolysis rate constants in the chemical mechanism. A zero-dimensional model treats the chemistry as a single system evolving in time and does not consider meteorology or boundary layer dynamics, but the relative simplicity of these models allows the use of a highly detailed chemical mechanism. The stagnant air and constrained meteorology in these valleys make this an appropriate technique for these conditions (Edwards et al., 2014). Further model details are described in Text S3 (de Gouw et al., 2017; Kurtenbach et al., 2001; McDuffie, 2018; Wesely & Hicks, 2000; Wild et al., 2017; Zhang et al., 2012).
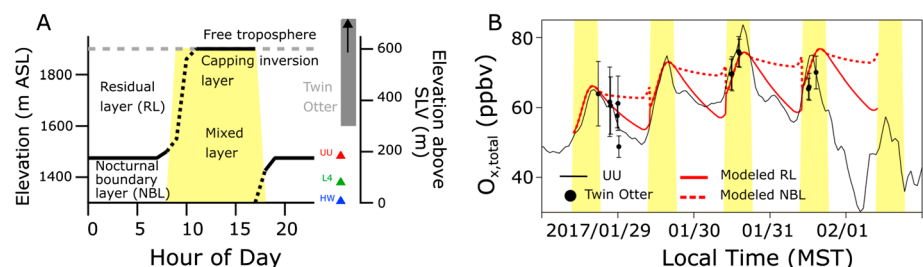
3. Results

Figure 2a shows the most abundant components of $O_{x,total}$ observed at the UU sampling site during the UWFPS campaign. As the PCAP progressed, $O_{x,total}$ increased steadily at a rate of approximately 5.5 ppbv/day, and its composition quickly became dominated by NO_2 and pNO_3^-. A similar trend is observed in Twin Otter vertical profiles (Figure 2b). These observations of $O_{x,total}$ growth and partitioning are compared to a recent study in the nearby Uintah Basin that also experiences frequent wintertime PCAPs (Ahmadov et al., 2015). In contrast to SLV, the sparsely populated Uintah Basin in northeastern Utah experiences high wintertime levels of O_3 (UBWOS, 2014) due to photochemical oxidation of VOCs emitted in abundance from local oil and natural gas operations in a relatively NO_x-poor environment (Edwards et al., 2014). Figure 2c shows a similar growth rate of $O_{x,total}$ in the Uintah Basin in during a PCAP in January 2013, but unlike the SLV, $O_{x,total}$ in the Uintah Basin is partitioned nearly entirely to O_3. The SLV is densely populated and contains no oil and natural gas wells, though it does have significant agricultural and industrial sectors, and NO_x and VOC emission profiles typical of U.S. urban areas (Figure S3a). The closely related $O_{x,total}$ growth in Figure 2 is reflective of the same photochemical mechanisms playing important roles in both valleys (Kleeman et al., 2005; Meng et al., 1997; Nguyen & Dabdub, 2002), and the widely divergent partitioning of its components to either pNO_3^- in the SLV or O_3 in the Uintah Basin derives from their starkly different emission profiles (Figure S3b). The common parameter $O_{x,total}$ can therefore be used to evaluate mitigation strategies for controlling both criteria pollutants, as demonstrated below.

The production of tropospheric O_3, frequently the major component of $O_{x,total}$, is often evaluated in terms of its nonlinear sensitivity to NO_x and VOC emissions (Lin et al., 1988; Milford et al., 1989; Seinfeld, 1989; Trainer et al., 1993). Because small changes in the availability of NO_x can change the relative branching of the HO_x radical reaction pathways, the O_3 production rate and yield may either increase or decrease with NO_x availability, depending on the VOC concentration and composition (Lin et al., 1988), which often requires detailed modeling to characterize fully. Edwards et al. (2014) used a zero-dimensional box model to show that O_3 production in the Uintah Basin was close to its maximum efficiency with respect to NO_x at the prevailing VOC concentrations in winter. Here we develop an analogous model to explain the growth of $O_{x,total}$ in the SLV. We modified the DSMACC box model to split into two concurrent boxes at night to model the residual layer (RL) and nocturnal boundary layer (NBL) separately, to more accurately model the vertical structure of the PCAP, as shown in Figure 3a.
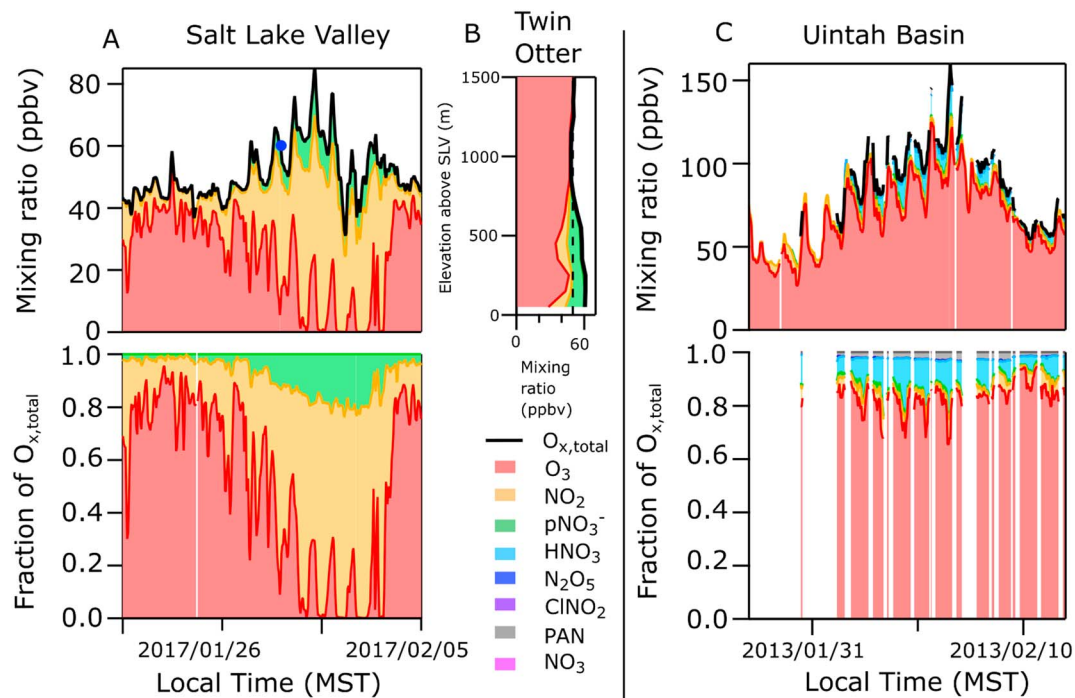
Figure 2. $O_{x,total}$ measured during the Utah Winter Fine Particulate Study 2017 and Uintah Basin Winter Ozone Study 2013 campaigns. (a) $O_{x,total}$ measured at the University of Utah ground site in the Salt Lake Valley during the UWFPS campaign with the major measured components of $O_{x,total}$ in filled colors. O_3 and NO_2 were the only components of $O_{x,total}$ directly measured at University of Utah, so pNO_3^- was calculated from the total particulate matter smaller than 2.5 microns in diameter measurement. The other gas-phase components were estimated to be minor contributors. When the persistent cold air pool (PCAP) begins on 26 January, a steady increase in $O_{x,total}$ is observed, along with a change in its partitioning, with NO_2 and pNO_3^- dominating and O_3 being depleted. (b) A vertical profile of the boundary layer on 28 January (denoted by blue circle in (a) from the Twin Otter. The height of the boundary layer is approximately 800-m above ground level, and $O_{x,total}$ remains at 50 ppbv above that height and grows well in excess of that budget beneath it. (c) The $O_{x,total}$ measured during the 2013 Uintah Basin Winter Ozone Study campaign in Uintah Basin, with some missing data due to instrument downtime. The PCAP begins on 29 January 2013 and persists for 9 days. In stark contrast to the Salt Lake Valley, O_3 represents approximately 85% of the $O_{x,total}$ throughout the PCAP in the Uintah Basin.

Figure 3b shows the base case model compared with the observations. The base case was selected based on daytime agreement between modeled and observed $O_{x,total}$, VOCs, and NO_x, as detailed in Text S3. The model did not attempt to replicate the partitioning of HNO_3 between the gas and aerosol phase and simply treated the two as the lumped sum $HNO_3 + pNO_3^-$. Franchin et al. (2018) showed this partitioning to be >92% to the aerosol phase during UWFPS PCAP events. The UU site is located at slightly higher elevation

Figure 3. Results of the photochemical box model of $O_{x,total}$ growth. (a) An idealized representation of the daily evolution of the pollution layer as implemented in the model. The gray dashed line shows the top of the capping inversion layer. The black line shows the nighttime division of the layer into a NBL and a RL. During the day, weak solar heating convectively mixes the two layers (black dashed lines). The elevation of the three ground sites above the SLV floor and the Twin Otter's cruising altitude range are on the right. (b) Comparison between model prediction and the UU observations of $O_{x,total}$. Emission rates were tuned such that the daytime (yellow rectangles) agreement between the modeled and observed $O_{x,total}$ was optimized. The location of the UU site on the valley wall is consistent with the nighttime measurement lying between the prediction for the RL and the NBL. SLV = Salt Lake Valley; UU = University of Utah.
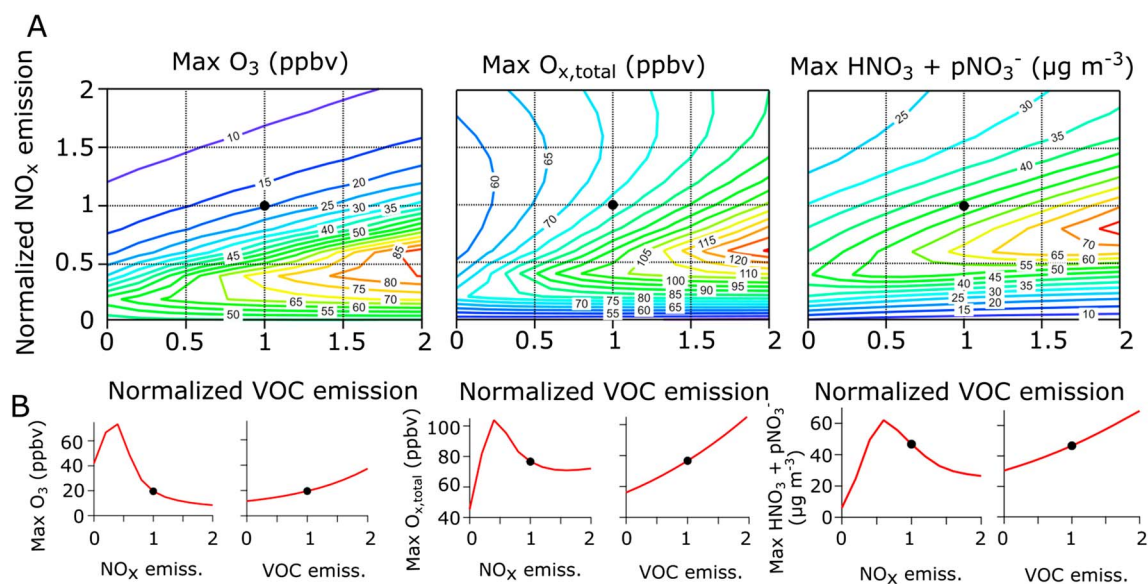
Figure 4. Isopleths of O_3, $O_{x,total}$, and $HNO_3 + pNO_3^-$ formation. (a) Isopleths of the predicted maximum daytime O_3, $O_{x,total}$, and $HNO_3 + pNO_3^-$ on the final day of the model in the Salt Lake Valley, as a function of normalized NO_x and VOC emissions. The black circles indicate the base case, and the contours show the predicted maximum concentration of each species as the normalized emissions are varied between 0 and 2. (b) Cuts through each isopleth at the base case, with normalized NO_x and VOC emissions of 1. VOC = volatile organic compound.

on the side of the valley wall and may sample from either the NBL or RL at night at different times during the PCAP (see Text S3.1). Additionally, that site may be subject to upslope and downslope canyon flows along the basin walls (Baasandorj et al., 2017). Agreement between the model and UU observations was therefore only expected during daytime hours when the pollution layer is mixed. The split box model successfully captures the overall growth of $O_{x,total}$ over the four model days, accurately predicts that there is O_3 depletion in the NBL due to dilution and reaction with NO_2 but not in the RL, and reproduces the observed partitioning of $O_{x,total}$ (Figure S4).

The input emission rates may be adjusted from the model base case to determine the effect of various emission control strategies. Isopleths determined in this way are often used to predict the effect of emission controls on O_3 production (Kleinman, 2005; Seinfeld, 1989). VOC controls on $PM_{2.5}$ formation have been considered in the past in California (Kleeman et al., 2005; Nguyen & Dabdub, 2002; Pun & Seigneur, 2001). However, VOC controls in the context of the chemical equivalence of O_3 and pNO_3^- in terms of $O_{x,total}$ during weak photochemical environments, such as the SLV, have not been considered. Calculated isopleths of O_3, $O_{x,total}$, and the sum of $HNO_3 + pNO_3^-$ are shown in Figure 4. They indicate that the SLV is in a NO_x-saturated regime, where initial decreases in NO_x emissions will increase O_3, $O_{x,total}$, and $HNO_3 + pNO_3^-$, absent concurrent VOC reductions.

NO_x saturation in the SLV is attributed to the modeled average HO_x chain length or the number of times a HO_x radical undergoes a propagation reaction cycle generating NO_2 before terminating (Jeffries & Tonnesen, 1994; Mao et al., 2010). The model predicts this value to be 1.07 in the SLV (Figure S5), so HO_x is near its peak efficiency for HNO_3 production, as over 99% of HO_x radicals terminate in HNO_3, rather than an alkyl nitrate or HO_x self-reaction. This observation is also consistent with the low observed aerosol-phase organic nitrates (Franchin et al., 2018). NO_x serves to quench the HO_x-NO_x cycle, and therefore, reductions in NO_x increase the HO_x chain length and drive more efficient production of O_3 and HNO_3. In the Uintah Basin, on the other hand, the average chain length is 4.3, indicating that HO_x radicals are highly efficient in generating O_3 before termination largely via self-reaction. The ratio of NO_x to VOCs (Figure S3b) is a key parameter that dictates the ultimate fate of radicals: High NO_x/VOCs yields high HNO_3 in the SLV, whereas low NO_x/VOC yields high O_3 in Uintah Basin.

It is often assumed that when pNO_3^- production is HNO_3-limited (as opposed to NH_3-limited), HNO_3 production must be NO_x-limited (Guo et al., 2018; Wen et al., 2018), and previous studies in California's San

AGU
100
ADVANCING EARTH
AND SPACE SCIENCE

Geophysical Research Letters

10.1029/2019GL082028

Joaquin Valley have found that >50% NO_x reductions would reduce pNO_3^- (Kelly et al., 2018; Pusede et al., 2016). However, Figure 4 demonstrates that the SLV is HNO_3-limited and NO_x-saturated simultaneously (see also Pun & Seigneur, 2001). Our finding implies a counterintuitive control strategy to initially reduce VOC emissions could be more effective in controlling ammonium nitrate aerosol exceedances in the NO_x-rich SLV, though a combination of NO_x and VOC control will eventually be necessary for reduction below U.S. air quality standards. The model can also elucidate the relative roles of the daytime and nighttime chemical mechanisms for forming HNO_3. We derive a 43% contribution to total HNO_3 formation by nighttime N_2O_5 uptake on aerosol (Figure S6), with nighttime HNO_3 production occurring primarily in the RL, where there are no NO_x emissions.

4. Conclusions

$O_{x,total}$ is a parameter that describes both O_3 and pNO_3^- production, demonstrating that they are different outcomes of the same chemical cycle, driven by different NO_x/VOC emission ratios, and may be considered chemically equivalent. We have therefore modeled the predicted response of $O_{x,total}$ to changes in NO_x and VOC emissions in the same manner that O_3 production is normally considered. Although this conceptual model is simplified, its conclusions are robust with respect to the underlying assumptions, as detailed in sensitivity tests in Text S4 (Li et al., 2014; Stemmler et al., 2006; Zhou et al., 2011). We find that this framework is an effective way of describing the response of ammonium nitrate aerosol to emission controls in an urban wintertime environment that is sensitive to HNO_3. Furthermore, a more general three-component analysis which considers NO_x, VOCs, and NH_3 could describe ammonium nitrate formation under any conditions in the context of $O_{x,total}$. We find that the SLV is likely to be well within a NO_x-saturated regime, and therefore, control strategies that initially focus on VOCs rather than NO_x or NH_3 would be most effective, contrary to the view that NO_x reductions are most effective in HNO_3 (rather than NH_3) limited systems. The current understanding of U.S. VOC emissions and the cost and feasibility of their reduction continues to evolve (McDonald et al., 2018). Further detailed evaluation of the unique and changing biogenic and anthropogenic VOC profiles in the SLV and other valleys would be required to formulate an effective VOC emission control strategy.

Recent work has noted that summertime O_3 and $PM_{2.5}$ in the United States have steadily declined (Cooper et al., 2014; Hand et al., 2014) in response to emissions controls, but wintertime $PM_{2.5}$, nitrate aerosol in particular, has not decreased as strongly (Green et al., 2015; Shah et al., 2018). Our analysis further suggests that these more gradual decreases in western U.S. $PM_{2.5}$ may be attributable to recent reductions in VOC rather than NO_x emissions and that NO_x reductions may in fact have had the counterintuitive effect of slowing the rate of decrease of $PM_{2.5}$ in areas dominated by ammonium nitrate. This analysis may also be relevant to both Europe and East Asia (Figure 1), where nitrate is increasingly a major component of wintertime $PM_{2.5}$ (Xu et al., 2018), NO_x concentrations are high (Guo et al., 2014; Wang et al., 2017, 2018; Wen et al., 2018), and ammonia is typically in excess (Guo et al., 2018). Mitigation strategies have normally focused on NO_x control (Guo et al., 2018), though recent work has indicated that $PM_{2.5}$ in northern China has a negative sensitivity to NO_x (Zhao et al., 2017). Chinese emission inventories show recent reductions in NO_x but increase in VOCs nationwide, a trend that could serve to exacerbate the severity of nitrate aerosol (Wang et al., 2017). Although the NO_x and VOC emission profiles in European and Chinese cities may differ substantially from valleys in northern Utah, this framework for modeling aerosol suggests new and promising avenues for improved control strategies.

References

Ahmadov, R., McKeen, S., Trainer, M., Banta, R., Brewer, A., Brown, S., et al. (2015). Understanding high wintertime ozone pollution events in an oil- and natural gas-producing region of the western US. *Atmospheric Chemistry and Physics*, 15(1), 411–429. https://doi.org/10.5194/acp-15-411-2015

Baasandorj, M., Brown, S. S., Hoch, S., Crosman, E., Long, R., Silva, P., et al. (2018). 2017 Utah Winter Fine Particulate Study Final Report. Retrieved from https://www.esrl.noaa.gov/csd/groups/csd7/measurements/2017uwfps/finalreport.pdf

Baasandorj, M., Hoch, S. W., Bares, R., Lin, J. C., Brown, S. S., Millet, D. B., et al. (2017). Coupling between chemical and meteorological processes under persistent cold-air pool conditions: Evolution of wintertime $PM_{2.5}$ pollution events and N_2O_5 observations in Utah's Salt Lake Valley. *Environmental Science & Technology*, 51(11), 5941–5950. https://doi.org/10.1021/acs.est.6b06603

Bares, R., Lin, J. C., Hoch, S. W., Baasandorj, M., Mendoza, D. L., Fasoli, B., et al. (2018). The wintertime covariation of CO_2 and criteria pollutants in an urban valley of the Western United States. *Journal of Geophysical Research: Atmospheres*, *123*, 2684–2703. https://doi.org/10.1002/2017JD027917

Beard, J. D., Beck, C., Graham, R., Packham, S. C., Traphagan, M., Giles, R. T., & Morgan, J. G. (2012). Winter temperature inversions and emergency department visits from asthma in Salt Lake County, Utah, 2003–2008. *Environmental Health Perspectives*, *120*(10), 1385–1390. https://doi.org/10.1289/ehp.1104349

Blanchard, C. L., Roth, P. M., Tanenbaum, S. J., Ziman, S. D., & Seinfeld, J. H. (2000). The use of ambient measurements to identify which precursor species limit aerosol nitrate formation. *Journal of the Air & Waste Management Association*, *50*(12), 2073–2084. https://doi.org/10.1080/10473289.2000.10464239

Cooper, O. R., Parrish, D. D., Ziemke, J., Balashov, N. V., Cupeiro, M., Galbally, I. E., et al. (2014). Global distribution and trends of tropospheric ozone: An observation-based review. *Elementa: Science of the Anthropocene*, *2*(29). https://doi.org/10.12952/journal.elementa.000029

de Gouw, J. A., Gilman, J. B., Kim, S. W., Lerner, B. M., Isaacman-VanWertz, G., McDonald, B. C., et al. (2017). Chemistry of volatile organic compounds in the Los Angeles basin: Nighttime removal of alkenes and determination of emission ratios. *Journal of Geophysical Research: Atmospheres*, *122*, 11,843–11,861. https://doi.org/10.1002/2017JD027459

DOS (2018). US Department of State. Mission China Air Quality Monitoring Program Archive. Retrieved from https://www.stateair.net/web/historical/1/1.html, Accessed September 5, 2018.

Edwards, P. M., Brown, S. S., Roberts, J. M., Ahmadov, R., Banta, R. M., deGouw, J. A., et al. (2014). High winter ozone pollution from carbonyl photolysis in an oil and gas basin. *Nature*, *514*(7522), 351–354. https://doi.org/10.1038/nature13767

EMEP (2018). European Monitoring and Evaluation Programme. Norwegian Institute for Air Research EBAS [internet database]. Retrieved from https://ebas.nilu.no/Default.aspx, Accessed December 11, 2018.

Emmerson, K. M., & Evans, M. J. (2009). Comparison of tropospheric gas-phase chemistry schemes for use within global models. *Atmospheric Chemistry and Physics*, *9*(5), 1831–1845. https://doi.org/10.5194/acp-9-1831-2009

EPA (2018). US Environmental Protection Agency. Air Quality System Data Mart [internet database]. Retrieved from. https://www.epa.gov/ttn/airs/aqsdatamart, Accessed September 5, 2018.

Franchin, A., Fibiger, D. L., Goldberger, L., McDuffie, E. E., Moravek, A., Womack, C. C., et al. (2018). Airborne and ground-based observations of ammonium nitrate dominated aerosols in a shallow boundary layer during intense winter pollution episodes in northern Utah. *Atmospheric Chemistry and Physics*, *18*(23), 17,259–17,276. https://doi.org/10.5194/acp-18-17259-2018

Green, M. C., Chow, J. C., Watson, J. G., Dick, K., & Inouye, D. (2015). Effects of snow cover and atmospheric stability on winter $PM_{2.5}$ concentrations in Western U.S. valleys. *Journal of Applied Meteorology and Climatology*, *54*(6), 1191–1201. https://doi.org/10.1175/jamc-d-14-0191.1

Guo, H., Otjes, R., Schlag, P., Kiendler-Scharr, A., Nenes, A., & Weber, R. J. (2018). Effectiveness of ammonia reduction on control of fine particle nitrate. *Atmospheric Chemistry and Physics*, *18*(16), 12,241–12,256. https://doi.org/10.5194/acp-18-12241-2018

Guo, S., Hu, M., Zamora, M. L., Peng, J., Shang, D., Zheng, J., et al. (2014). Elucidating severe urban haze formation in China. *Proceedings of the National Academy of Sciences*, *111*(49), 17,373–17,378. https://doi.org/10.1073/pnas.1419604111

Hand, J. L., Schichtel, B. A., Malm, W. C., Copeland, S., Molenar, J. V., Frank, N., & Pitchford, M. (2014). Widespread reductions in haze across the United States from the early 1990s through 2011. *Atmospheric Environment*, *94*, 671–679. https://doi.org/10.1016/j.atmosenv.2014.05.062

Jeffries, H. E., & Tonnesen, S. (1994). A comparison of two photochemical reaction mechanisms using mass balance and process analysis. *Atmospheric Environment*, *28*(18), 2991–3003. https://doi.org/10.1016/1352-2310(94)90345-X

Jenkin, M. E., Young, J. C., & Rickard, A. R. (2015). The MCM v3.3.1 degradation scheme for isoprene. *Atmospheric Chemistry and Physics*, *15*(20), 11,433–11,459. https://doi.org/10.5194/acp-15-11433-2015

Jones, C. L., & Seinfeld, J. H. (1983). The oxidation of NO_2 to nitrate—Day and night. *Atmospheric Environment*, *17*(11), 2370–2373. https://doi.org/10.1016/0004-6981(83)90239-1

Kelly, J. T., Parworth, C. L., Zhang, Q., Miller, D. J., Sun, K., Zondlo, M. A., et al. (2018). Modeling NH_4NO_3 over the San Joaquin Valley during the 2013 DISCOVER-AQ Campaign. *Journal of Geophysical Research: Atmospheres*, *123*, 4727–4745. https://doi.org/10.1029/2018JD028290

Kelly, K. E., Kotchenruther, R., Kuprov, R., & Silcox, G. D. (2013). Receptor model source attributions for Utah's Salt Lake City airshed and the impacts of wintertime secondary ammonium nitrate and ammonium chloride aerosol. *Journal of the Air & Waste Management Association*, *63*(5), 575–590. https://doi.org/10.1080/10962247.2013.774819

Kleeman, M. J., Ying, Q., & Kaduwela, A. (2005). Control strategies for the reduction of airborne particulate nitrate in California's San Joaquin Valley. *Atmospheric Environment*, *39*(29), 5325–5341. https://doi.org/10.1016/j.atmosenv.2005.05.044

Kleinman, L. I. (2005). The dependence of tropospheric ozone production rate on ozone precursors. *Atmospheric Environment*, *39*(3), 575–586. https://doi.org/10.1016/j.atmosenv.2004.08.047

Kuprov, R., Eatough, D. J., Cruickshank, T., Olson, N., Cropper, P. M., & Hansen, J. C. (2014). Composition and secondary formation of fine particulate matter in the Salt Lake Valley: Winter 2009. *Journal of the Air & Waste Management Association*, *64*(8), 957–969. https://doi.org/10.1080/10962247.2014.903878

Kurtenbach, R., Becker, K. H., Gomes, J. A. G., Kleffmann, J., Lörzer, J. C., Spittler, M., et al. (2001). Investigations of emissions and heterogeneous formation of HONO in a road traffic tunnel. *Atmospheric Environment*, *35*(20), 3385–3394. https://doi.org/10.1016/S1352-2310(01)00138-8

Lee, B. H., Lopez-Hilfiker, F. D., Mohr, C., Kurtén, T., Worsnop, D. R., & Thornton, J. A. (2014). An iodide-adduct high-resolution time-of-flight chemical-ionization mass spectrometer: Application to atmospheric inorganic and organic compounds. *Environmental Science & Technology*, *48*(11), 6309–6317. https://doi.org/10.1021/es500362a

Li, X., Rohrer, F., Hofzumahaus, A., Brauers, T., Haseler, R., Bohn, B., et al. (2014). Missing gas-phase source of HONO inferred from zeppelin measurements in the troposphere. *Science*, *344*(6181), 292–296. https://doi.org/10.1126/science.1248999

Liao, J., Brock, C. A., Murphy, D. M., Sueper, D. T., Welti, A., & Middlebrook, A. M. (2017). Single-particle measurements of bouncing particles and in situ collection efficiency from an airborne aerosol mass spectrometer (AMS) with light-scattering detection. *Atmospheric Measurement Techniques*, *10*(10), 3801–3820. https://doi.org/10.5194/amt-10-3801-2017

Lin, X., Trainer, M., & Liu, S. C. (1988). On the nonlinearity of the tropospheric ozone production. *Journal of Geophysical Research*, *93*(D12), 15,879–15,888. https://doi.org/10.1029/JD093iD12p15879

Liu, S. C. (1977). Possible effects on tropospheric O_3 and OH due to NO emissions. *Geophysical Research Letters*, *4*(8), 325–328. https://doi.org/10.1029/GL004i008p00325

Madronich, S., McKenzie, R. L., Björn, L. O., & Caldwell, M. M. (1998). Changes in biologically active ultraviolet radiation reaching the Earth's surface. *Journal of Photochemistry and Photobiology B: Biology*, *46*(1-3), 5–19. https://doi.org/10.1016/S1011-1344(98)00182-1

Mao, J., Ren, X., Chen, S., Brune, W. H., Chen, Z., Martinez, M., et al. (2010). Atmospheric oxidation capacity in the summer of Houston 2006: Comparison with summer measurements in other metropolitan studies. *Atmospheric Environment*, *44*(33), 4107–4115. https://doi.org/10.1016/j.atmosenv.2009.01.013

McDonald, B. C., de Gouw, J. A., Gilman, J. B., Jathar, S. H., Akherati, A., Cappa, C. D., et al. (2018). Volatile chemical products emerging as largest petrochemical source of urban organic emissions. *Science*, *359*(6377), 760–764. https://doi.org/10.1126/science.aaq0524

McDuffie, E. (2018). Measurements and modeling of tropospheric transformations during summer and winter in polluted regions across the U.S., Doctoral dissertation thesis, University of Colorado, Boulder.

Meng, Z., Dabdub, D., & Seinfeld, J. H. (1997). Chemical coupling between atmospheric ozone and particulate matter. *Science*, *277*(5322), 116–119. https://doi.org/10.1126/science.277.5322.116

Milford, J. B., Russell, A. G., & McRae, G. J. (1989). A new approach to photochemical pollution control: Implications of spatial patterns in pollutant responses to reductions in nitrogen oxides and reactive organic gas emissions. *Environmental Science & Technology*, *23*(10), 1290–1301. https://doi.org/10.1021/es00068a017

Nguyen, K., & Dabdub, D. (2002). NO_x and VOC control and its effects on the formation of aerosols. *Aerosol Science and Technology*, *36*(5), 560–572. https://doi.org/10.1080/02786820252883801

Pun, B. K., & Seigneur, C. (2001). Sensitivity of particulate matter nitrate formation to precursor emissions in the California San Joaquin Valley. *Environmental Science & Technology*, *35*(14), 2979–2987. https://doi.org/10.1021/es0018973

Pusede, S. E., Duffey, K. C., Shusterman, A. A., Saleh, A., Laughner, J. L., Wooldridge, P. J., et al. (2016). On the effectiveness of nitrogen oxide reductions as a control over ammonium nitrate aerosol. *Atmospheric Chemistry and Physics*, *16*(4), 2575–2596. https://doi.org/10.5194/acp-16-2575-2016

Seinfeld, J. H. (1989). Urban air pollution: State of the science. *Science*, *243*(4892), 745–752. https://doi.org/10.1126/science.243.4892.745

Shah, V., Jaeglé, L., Thornton, J. A., Lopez-Hilfiker, F. D., Lee, B. H., Schroder, J. C., et al. (2018). Chemical feedbacks weaken the wintertime response of particulate sulfate and nitrate to emissions reductions over the eastern United States. *Proceedings of the National Academy of Sciences*, *115*(32), 8110–8115. https://doi.org/10.1073/pnas.1803295115

Silcox, G. D., Kelly, K. E., Crosman, E. T., Whiteman, C. D., & Allen, B. L. (2012). Wintertime $PM_{2.5}$ concentrations during persistent, multiday cold-air pools in a mountain valley. *Atmospheric Environment*, *46*, 17–24. https://doi.org/10.1016/j.atmosenv.2011.10.041

Stemmler, K., Ammann, M., Donders, C., Kleffmann, J., & George, C. (2006). Photosensitized reduction of nitrogen dioxide on humic acid as a source of nitrous acid. *Nature*, *440*(7081), 195–198. https://doi.org/10.1038/nature04603

Trainer, M., Parrish, D. D., Buhr, M. P., Norton, R. B., Fehsenfeld, F. C., Anlauf, K. G., et al. (1993). Correlation of ozone with NO_y in photochemically aged air. *Journal of Geophysical Research*, *98*(D2), 2917–2925. https://doi.org/10.1029/92JD01910

UBWOS (2014). Uinta Basin 2013 Winter Ozone Study: Final Report. Retrieved from https://deq.utah.gov/legacy/destinations/u/uintah-basin/ozone/strategies/studies/UBOS-2013.htm

Wang, H., Lu, K., Chen, X., Zhu, Q., Wu, Z., Wu, Y., & Sun, K. (2018). Fast particulate nitrate formation via N_2O_5 uptake aloft in winter in Beijing. *Atmospheric Chemistry and Physics*, *18*(14), 10,483–10,495. https://doi.org/10.5194/acp-18-10483-2018

Wang, J., Zhao, B., Wang, S., Yang, F., Xing, J., Morawska, L., et al. (2017). Particulate matter pollution over China and the effects of control policies. *Science of the Total Environment*, *584-585*, 426–447. https://doi.org/10.1016/j.scitotenv.2017.01.027

Weber, R. J., Guo, H., Russell, A. G., & Nenes, A. (2016). High aerosol acidity despite declining atmospheric sulfate concentrations over the past 15 years. *Nature Geoscience*, *9*(4), 282–285. https://doi.org/10.1038/ngeo2665

Wen, L., Xue, L., Wang, X., Xu, C., Chen, T., Yang, L., et al. (2018). Summertime fine particulate nitrate pollution in the North China Plain: Increasing trends, formation mechanisms and implications for control policy. *Atmospheric Chemistry and Physics*, *18*(15), 11,261–11,275. https://doi.org/10.5194/acp-18-11261-2018

Wesely, M. L., & Hicks, B. B. (2000). A review of the current status of knowledge on dry deposition. *Atmospheric Environment*, *34*(12), 2261–2282. https://doi.org/10.1016/S1352-2310(99)00467-7

Whiteman, C. D., Hoch, S. W., Horel, J. D., & Charland, A. (2014). Relationship between particulate air pollution and meteorological variables in Utah's Salt Lake Valley. *Atmospheric Environment*, *94*, 742–753. https://doi.org/10.1016/j.atmosenv.2014.06.012

Wild, R. J., Dubé, W. P., Aikin, K. C., Eilerman, S. J., Neuman, J. A., Peischl, J., et al. (2017). On-road measurements of vehicle NO_2/NO_x emission ratios in Denver, Colorado, USA. *Atmospheric Environment*, *148*, 182–189. https://doi.org/10.1016/j.atmosenv.2016.10.039

Wild, R. J., Edwards, P. M., Bates, T. S., Cohen, R. C., de Gouw, J. A., Dubé, W. P., et al. (2016). Reactive nitrogen partitioning and its relationship to winter ozone events in Utah. *Atmospheric Chemistry and Physics*, *16*(2), 573–583. https://doi.org/10.5194/acp-16-573-2016

Wild, R. J., Edwards, P. M., Dubé, W. P., Baumann, K., Edgerton, E. S., Quinn, P. K., et al. (2014). A measurement of total reactive nitrogen, NO_y, together with NO_2, NO, and O_3 via cavity ring-down spectroscopy. *Environmental Science & Technology*, *48*(16), 9609–9615. https://doi.org/10.1021/es501896w

Wood, E. C., Herndon, S. C., Onasch, T. B., Kroll, J. H., Canagaratna, M. R., Kolb, C. E., et al. (2009). A case study of ozone production, nitrogen oxides, and the radical budget in Mexico City. *Atmospheric Chemistry and Physics*, *9*(7), 2499–2516. https://doi.org/10.5194/acp-9-2499-2009

Xu, W., Sun, Y., Wang, Q., Zhao, J., Wang, J., Ge, X., et al. (2018). Changes in aerosol chemistry from 2014 to 2016 in winter in Beijing: Insights from high resolution aerosol mass spectrometry. *Journal of Geophysical Research: Atmospheres*, *124*, 1132–1147. https://doi.org/10.1029/2018JD029245

Zhang, L., Jacob, D. J., Knipping, E. M., Kumar, N., Munger, J. W., Carouge, C. C., et al. (2012). Nitrogen deposition to the United States: Distribution, sources, and processes. *Atmospheric Chemistry and Physics*, *12*(10), 4539–4554. https://doi.org/10.5194/acp-12-4539-2012

Zhao, B., Wu, W., Wang, S., Xing, J., Chang, X., Liou, K. N., et al. (2017). A modeling study of the nonlinear response of fine particles to air pollutant emissions in the Beijing–Tianjin–Hebei region. *Atmospheric Chemistry and Physics*, *17*(19), 12,031–12,050. https://doi.org/10.5194/acp-17-12031-2017

Zhou, X., Zhang, N., TerAvest, M., Tang, D., Hou, J., Bertman, S., et al. (2011). Nitric acid photolysis on forest canopy surface as a source for tropospheric nitrous acid. *Nature Geoscience*, *4*(7), 440–443. https://doi.org/10.1038/ngeo1164